Electronic Supplementary Material (ESI) for Nanoscale.

Supplementary Information

Development of Antifouling Interpenetrating Polymer Network Hydrogel Film for Saliva Glucose Monitoring

Zifeng Zhang[a,b], Qian Dou[a,b], Shiwen Wang[b], Debo Hu[b,c], Bei Yang[b,c], Zhipeng Zhao[b,c], Hongliang Liu*[d], Qing Dai*[a, b, c]

[a] *School of Materials Science and Engineering, Zhengzhou University, Zhengzhou 450001, P. R. China*

**E-mail: daiq@nanoctr.cn; liuhl@mail.ipc.ac.cn*

[b] *Division of Nanophotonics, CAS Key Laboratory of Standardization and Measurement for Nanotechnology, CAS Center for Excellence in Nanoscience, National Center for Nanoscience and Technology, Beijing 100190, P. R. China*

[c] *Center of Materials Science and Optoelectronics Engineering, University of Chinese Academy of Sciences, Beijing 100049, P. R. China*

[d] *Technical Institute of Physics and Chemistry, University of Chinese Academy of Sciences, Beijing 100190, P. R. China*

Table. S1 Elemental surface composition of SAM of initiator, polySBMA brushes, and IPN hydrogel film determined from XPS

Sample	Element (atom %)						
	C	O	S	N	Br	B	Au
SAM of initiator	69.175	6.657	2.882	------	0.194	------	21.093
polySBMA brushes	63.874	24.153	5.093	4.534	------	------	2.346
IPN hydrogel	69.623	16.733	0.162	12.167	------	1.315	------

Table. **S2** The % RSD of IPN hydrogel film after five association–dissociation cycles.

Film	Glucose level (mg/L)	Mean of glucose response (Hz)	Standard deviations	% RSD
IPN hydrogel	10	7.9	0.2	2.5%
	30	12	1.0	8.3%
	50	24.8	1.6	6.4%

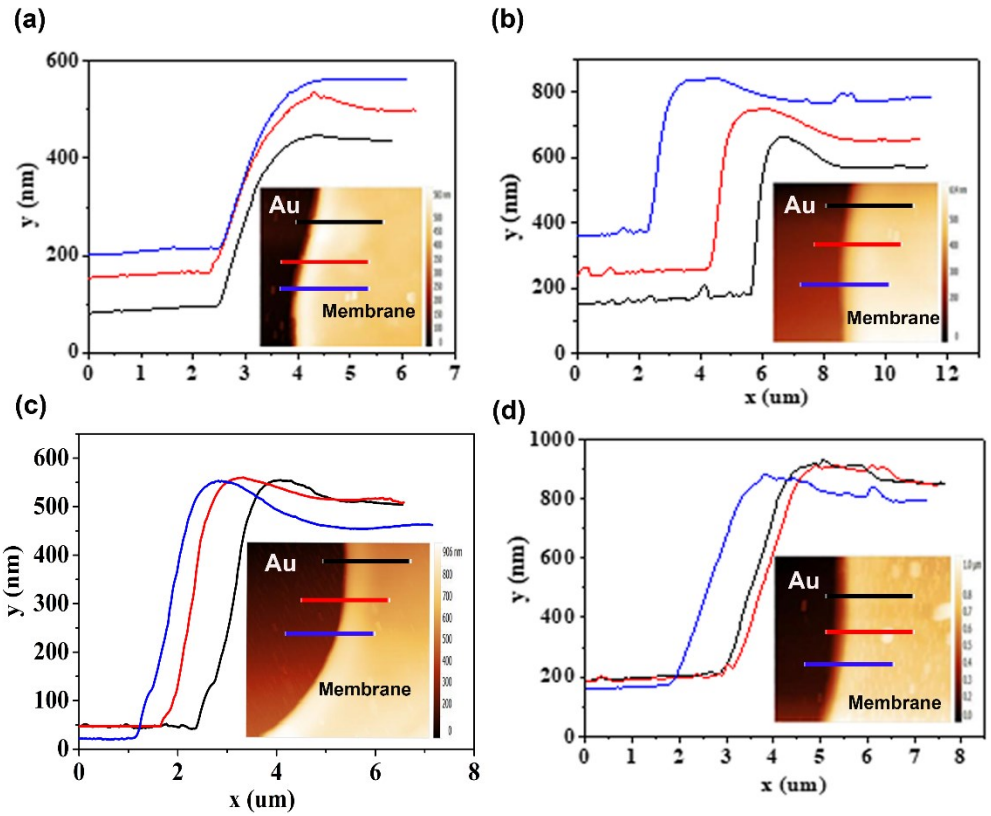

Fig. S1 The thickness of IPN hydrogel film obtained at different spinning speed.

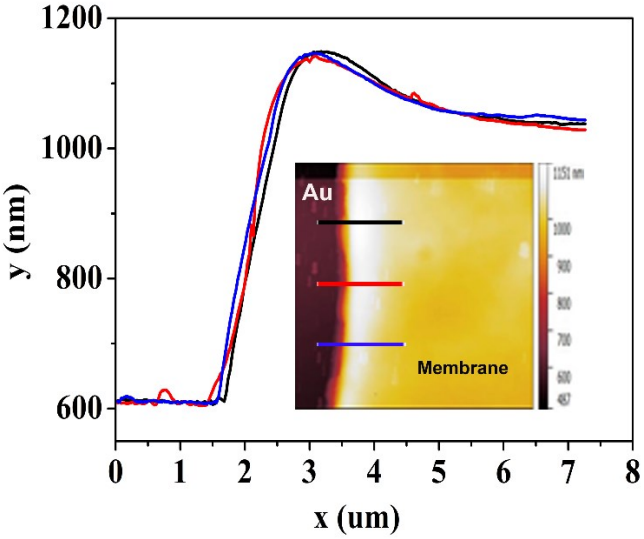

Fig. S2 The thickness of the PBA-functionalized hydrogel filmy

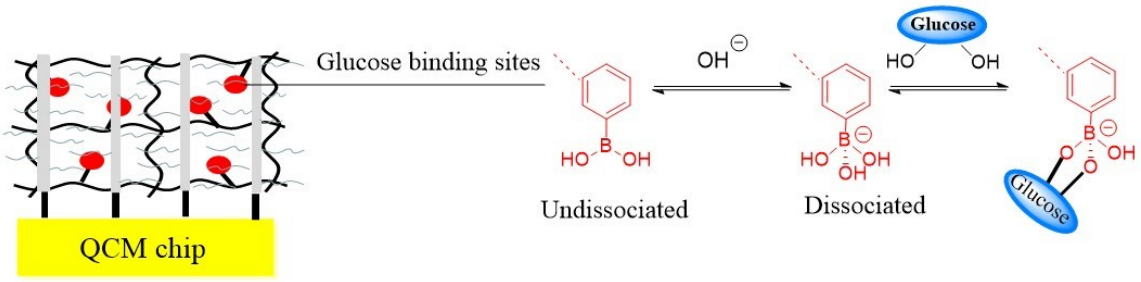

Fig. S3 The mechanism of glucose recognition between PBA and glucose molecules

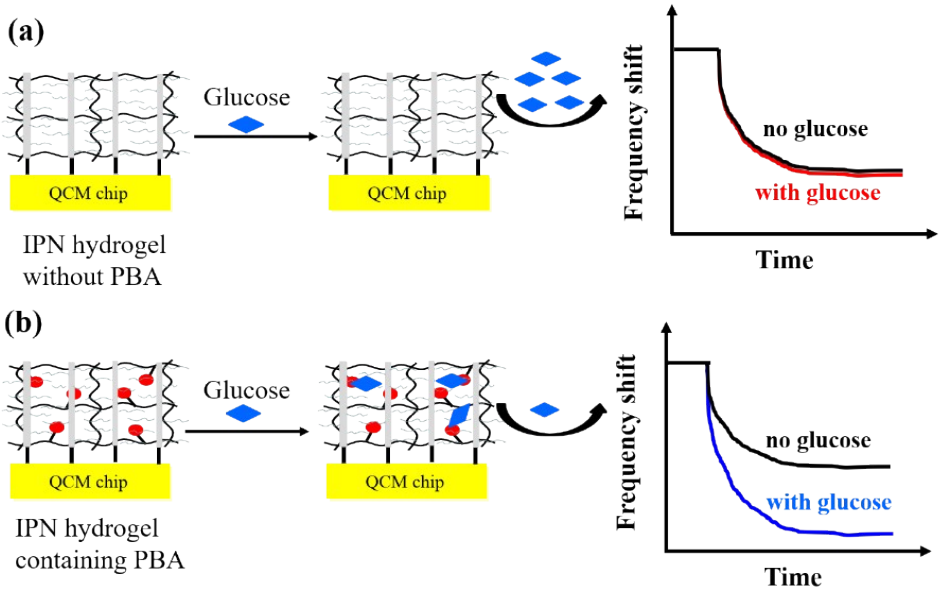

Fig. S4 (a) Glucose molecules cannot be recognized by IPN hydrogel film-coated QCM chip when no glucose-sensitive monomer (PBA) is added. It will not affect the frequency shift. (b) When glucose-sensitive PBA is added, the IPN hydrogel film-coated QCM chip can effectively

recognize the glucose molecules. It will cause an increase in frequency shift.

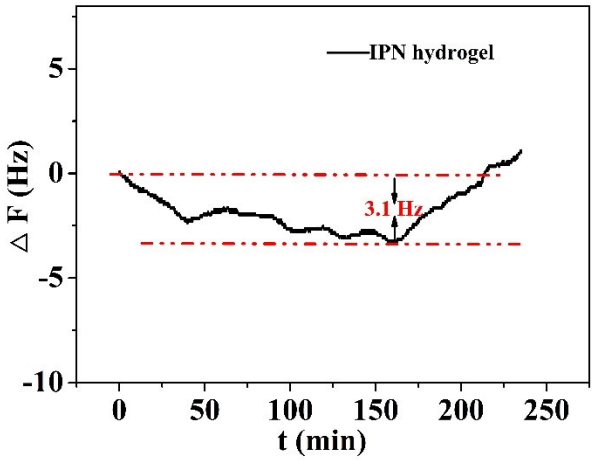

Fig. S5 The stability of IPN hydrogel film-coated QCM sensor in PBS solution at pH=7.5

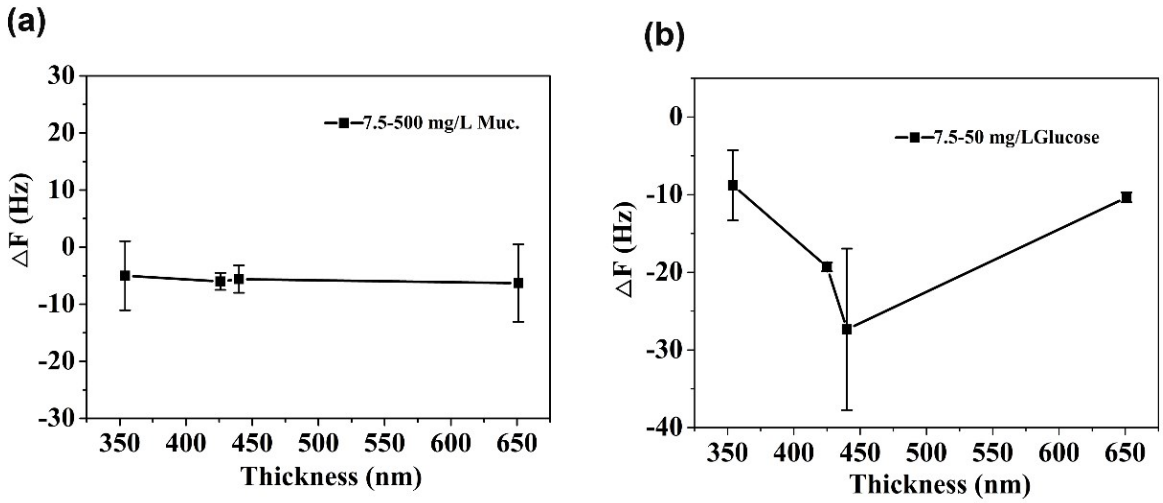

Fig. S6 (a) Fouling from 500 mg/L Muc. on different thickness of IPN hydrogel film. (b) Glucose response of different thickness of IPN hydrogel film.

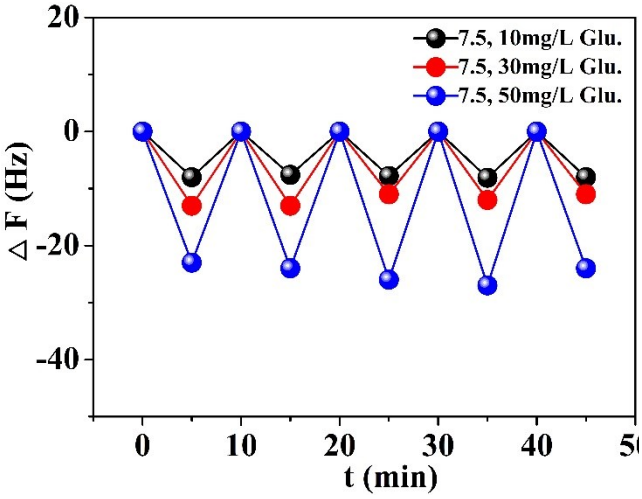

Fig. S7 Repeatability of IPN hydrogel film

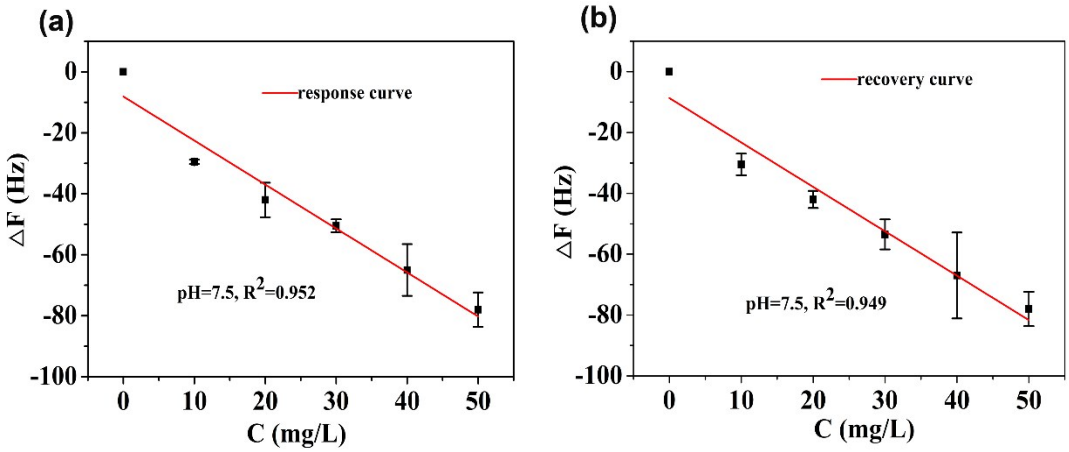

Fig. S8 Relationship of response and recovery behaviour between frequency shift and glucose concentration in diluted saliva, pH=7.5

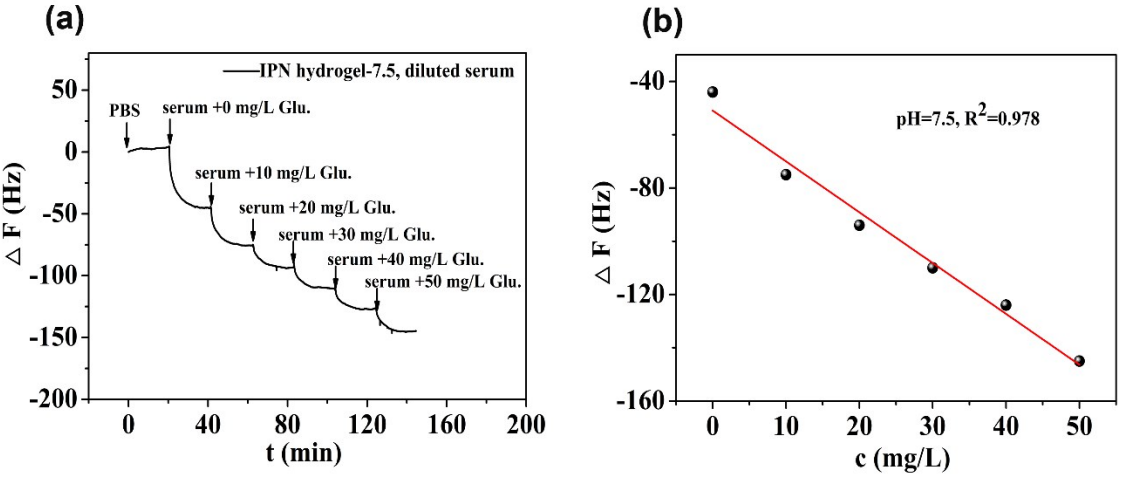

Fig. S9 (a) The detection of glucose in diluted serum by IPN hydrogel film-coated QCM sensor. (b) Relationship between frequency shift and glucose concentration.

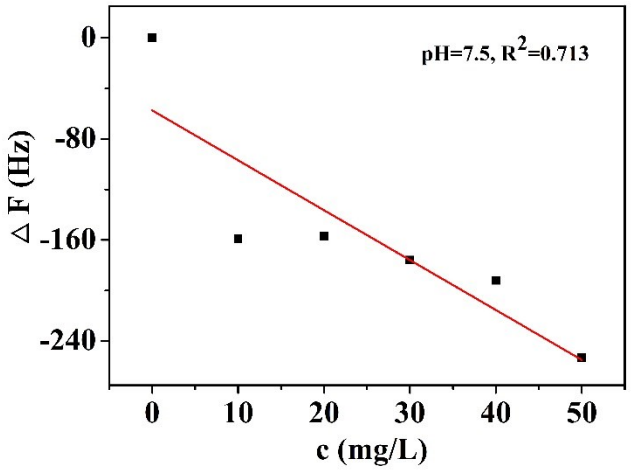

Fig. S10 Relationship between frequency shift and glucose concentration for PBA-functionalized hydrogel film-coated QCM sensor.

Table S3 show that the electrochemical glucose sensor can detect the glucose concentration in the blood glucose range. However, the glucose-sensitive material has not been treated with antifouling material and only the performance of high glucose levels in the serum (such as 6.22 and 9.44 mM) was tested.[3] The protein in real sample (such as serum, saliva) can bind nonspecifically and interfere or inhibit glucose-responsive materials/glucose interactions, thus produce false positive assay results. The traditional antifouling coating of biosensor such as electrochemical sensor can hinder the transport of glucose molecules owing to its steric hindrance, thus limiting its application in detection of low saliva glucose levels. Moreover, the glucose-sensitive materials of the electrochemical glucose sensor are mainly focused on enzyme and noble metals. Owing to the intrinsic nature of enzymes, enzyme-based sensors always suffer from stability problems caused by temperature, pH, humidity and toxic chemicals. Noble metals (such as Pt, Au, and Pd) have the drawbacks of low sensitivity and poor selectivity, caused by surface poisoning from adsorbed intermediates (such as protein) and chloride.[4]

The glucose-sensitive materials are the key factors to determine the properties of QCM glucose sensor. The phenylboronic acid (PBA) is often used as the sensing materials for QCM glucose sensor, and it has excellent stability, durability and low cost compared with enzyme-based electrochemical and paper strip-based glucose sensor. In particular, PBA-containing hydrogels have high sensitively to glucose and offer biocompatibility, and have become a promising material for dynamic glucose monitoring. For example, in our recent work, PBA-containing hydrogel-

coated QCM sensor realized a detection range of 10 – 5994 mg/L and response time of 100 s, which could fulfill the requirement of physiological range of blood glucose concentration in 7.5 PBS solution.[17] In this work, we developed a novel hydrogel film that enhanced the antifouling and sensitivity of the QCM sensor by infiltrating glucose-sensitive monomer (i.e., PBA) into zwitterionic polymer brushes matrix to form interpenetrating polymer network (IPN). The IPN hydrogel film could detect the typical saliva glucose level (0 - 50 mg/L) in diluted saliva. Moreover, the storage condition of IPN hydrogel film is simple and convenient (such as distilled water, room temperature), which avoid the harsh storage condition of enzyme-based glucose sensors. Obviously, these excellent performances (such as antifouling, glucose sensitivity and simple storage condition) demonstrates that the proposed QCM sensor can potentially be applied to detect glucose in complex biological samples such as saliva, serum.

Table. S3 Comparison of analytical properties of the QCM glucose sensor with other detection methods

Detection method	Glucose-responsive material	Detection range	Limit of detection	Response time	Specimen	Reference
Electrochemical	MnO_2/MWNTs	1.8 - 5040 mg/L	------	10 s	0.1 M NaOH	1
	Pt-Pb	0 - 3600 mg/L	------	------	7.4 PBS	2
	GOx	1.8 – 1440 mg/L	0.126 mg/L	3 s	5.6 PBS	3
	$NiMoO_4$	9 – 2520 mg/L	0.0648 mg/L	4 s	1.2 M NaOH, 100% human serum	4
	GOx	18 – 3240 mg/L	156.6 mg/L	15 min	PBS, 100% human serum	5
Optical	GOx	0 – 540 mg/L	36 mg/L	------	7.0 PBS, 20% human serum	6

	PBA	0 – 1800 mg/L	------	0.47 min	8.5 PBS	7
	GOx	0 – 360 mg/L	0.09 mg/L	30 min	7.4 PBS, 10% serum	8
	PBA	540 – 3600 mg/L	------	------	8.0 – 8.5 CHES buffer	9
	PBA	0 – 18000 mg/L	------	90 min	7.4 PBS	10
	BA	0 – 180 mg/L	------	60 min	7.4 TES buffer, photosynthetic organism	11
	GOx-HPR	54 – 180 mg/L	38 mg/L	30 min	7.0 PBS, 100% human serum	12
	GOx-HPR	180 – 1980 mg/L	54 mg/L	6 min	7.0 PBS, 100% human serum	13
Paper strip	GOx	90 - 13500 mg/L	222 mg/L	45 s	7.0 PBS, 100% saliva	14
	GOx	18 – 3600 mg/L	1.8 mg/L	5 min	7.4 PBS, 100% human serum	15
	GOx-HPR	10 – 225 mg/L	3.7 mg/L	------	6.0 PBS, 100% human saliva	16
	PBA	10 – 5994 mg/L	------	100 s	7.5 PBS	17
QCM	ConA	1.8 – 1350 mg/L	0.9 mg/L (3δ)	------	Distilled water, cattle serum	18
	PBA	900 – 9000 mg/L	------	------	9.0 PBS	19
	CP	1.8 – 3600 mg/L	------	30 min	7.4 PBS, 10%	20

PBA	1 – 36 mg/L	1 mg/L	5 min	human serum 7.5 PBS	21
PBA	0 – 50 mg/L	10 mg/L	2 min	7.5 PBS, 10% saliva, 1% diluted serum	Our work

Reference:

1 J. Chen, W. D. Zhang and J. S. Ye, Electrochem. Commun., 2008, **10**, 1268-1271.

2 J. P. Wang, D. F. Thomas and A. Chen, Anal. Chem., 2008, **80**, 997-1004.

3 D. Y. Zhai, B. R. Liu, Y. Shi, L. J. Pan, Y. Q. Wang, W. B. Li, R. Zhang and G. H. Yu, ACS Nano, 2013, **7**, 3540-3546.

4 D. D. Wang, D. P. Cai, H. Huang, B. Liu, L. L. Wang, Y. Liu, H. Li, Y. R. Wang, Q. H. Li and T. H. Wang, Nanotechnol., 2015, **26**, 145501-145508.

5 J. Xu, K. K. Xu, Y. Han, D. Wang, X. Li, T. Hu, H. Yi and Z. H. Ni, Analyst, 2020, **145**, 5141-5147.

6 X. D. Wang, H. X. Chen, T. Y. Zhou, Z. J. Lin, J. B. Zeng, Z. X. Xie, X. Chen, K. Y. Wong, G. N. Chen and X. R. Wang, Biosens. Bioelectron., 2009, **24**, 3702-3705.

7 X. Zhang, Y. Guan and Y. J. Zhang, Biomacromolecules, 2012, **13**, 92-97.

8 H. L. He, X. L. Xu, H. X. Wu and Y. D. Jin, Adv. Mater., 2012, **24**, 1736-1740.

9 X. D. Hong, Y. Peng, J. L. Bai, B. A. Ning, Y. Y. Liu, Z. J. Zhou and Z. X. Gao, Small, 2014, **10**, 1308-1313.

10 M. Elsherif, M. U. Hassan, Ali. K. Yetisen and H. Butt, ACS Nano, 2018, **12**, 2283-2291.

11 J. M. Li, H. H. Wu, I. Santana, M. Fahlgren and J. P. Giraldo, ACS Appl. Mater. Interfaces, 2018, **10**, 28279-28289.

12 X. Chen, J. Chen, F. B. Wang, X. Xiang, M. Luo, X. H. Ji and Z. K. He, Biosens. Bioelectron., 2012, **35**, 363-368.

13 W. J. Zhu, D. Q. Feng, M. Chen, Z. D. Chen, R. Zhu, H. L. Fang and W. Wang, Sens. Actuators, B, 2014, **190**, 414-418.

14 A. Soni and S. K. Jha, Biosens. Bioelectron., 2015, **67**, 763-768.

15 W. Y. Li, S. Y. Lu, S. J. Bao, Z. Z. Shi, Z. S. Lu, C. M. Li and L. Yu, Biosens. Bioelectron., 2018, **99**, 603-611.

16 Luis A. S. Jimenez, A. M. Lucero, V. Osuna, I. E. Moreno and R. B. Dominguez, sensors, 2018, **18**, 1071-1077.

17 Q, Dou, D. B. Hu, H. K. Gao, Y. M. Zhang, A. K. Yetisen, H. D. Butt, J. Wang, G. J. Nie and Q. Dai, RSC Adv., 2017, **7**, 41384-42390.

18 D. P. Tang, Q. F. Li, J. Tang, B. L. Su and G. N. Chen, Anal. Chim. Acta., 2011, **686**, 144-149.

19 C. Sugnaux, H. A. Klok, Macromol. Rapid Commun, 2014, **35**, 1402-1407.

20 C. Li, X. Chen, F. Y. Zhang, X. X. He, G. Z. Fang, J. F. Liu and S. Wang, Anal. Chem., 2017, **89**, 10431-10438.

21 Z. Z. Zhang, Q. Dou, S. W. Wang, D. B. Hu, X. D. Guo, B. X. Liao, Z. P. Zhao, H. L. Liu and Q. Dai, J. Mater. Chem. C, 2020, **8**, 9655-9662.